Article

High Frequency (HF) Radar Detection of the Weak 2012 Indonesian Tsunamis

Belinda Lipa [1,*]**, Donald Barrick** [2]**, Subandono Diposaptono** [3]**, James Isaacson** [4]**, Basanta Kumar Jena** [5]**, Bruce Nyden** [2]**, Kuppili Rajesh** [6] **and T. Srinivasa Kumar** [6]

[1]   Codar Ocean Sensors, 125 La Sandra Way, Portola Valley, CA 94028, USA

[2]   Codar Ocean Sensors, 1914 Plymouth St., Mountain View, CA 94043, USA;
     E-Mails: Don@codar.com (D.B.); Bruce@codar.com (B.N.)

[3]   Ministry of Marine Affairs and Fisheries, Gedung Mina Bahari III Lt. 9 Jln. Medan Merdeka Timur
     No. 16, Jakarta Pusat, Indonesia; E-Mail: Subandono.diposaptono@yahoo.com

[4]   Codar Ocean Sensors, 5 Sunset Trail, Sunset Valley, TX 78745, USA;
     E-Mail: jisaac@Austin.rr.com

[5]   National Institute of Ocean Technology, Velachery-Tambaram Main Road, Narayanapuram,
     Pallikaranai, Chennai 600 100, Tamil Nadu, India; E-Mail: bkjena@niot.res.in

[6]   Indian National Centre for Ocean Information Services, "Ocean Valley", Paragathi Nagar (BO),
     Nizampet (SO), Hyderabad 500090, India; E-Mails: rajesh@incois.gov.in (K.R.);
     srinivas@incois.gov.in (T.S.K.)

*   Author to whom correspondence should be addressed; E-Mail: Belinda@lipa.name;
    Tel.: +1-650-851-5517; Fax: +1-408-773-0514.

Abstract: We report here on the observation and offline detection of the weak tsunamis generated by earthquakes near Indonesia on 11 April 2012 using radar systems and tide gauges on the coasts of Sumatra and the Andaman Islands. This work extends the previous observations of the much stronger 2011 Japan tsunami. The distance offshore at which the tsunami can be detected, and hence the warning time provided, depends primarily on the bathymetry: the wider the shallow continental shelf, the greater this time. The weak Indonesia tsunamis were detected successfully in spite of the narrow shallow-water shelf offshore from the radar systems. Larger tsunamis could obviously be detected further from the coast. This paper provides further confirmation that radar is an important tool to aid in tsunami observation and warning.

1. Introduction

Tsunami watch systems presently in place are based on computer models. They provide warning of earthquake-generated tsunami impacts, and predict their strength and arrival times *vs.* location based on the earthquake characteristics [1–3]. Seismic data and tsunami model predictions are disseminated rapidly after dangerous earthquakes. To date no system has been deployed which can detect an incoming tsunami with a significant warning capability. Tide-gauge sea levels at coastal positions closer to the epicenter can provide useful information on water levels for locations further downstream, if they are able to transmit data. The 2011 Japan tsunami signal was observed by many HF radars around the Pacific Rim with clear results from sites in Japan, US and Chile [4,5]. In addition to their primary operational purpose of observing real-time offshore circulation [6,7], the radars can also provide local quantitative tsunami information and warning as the actual wave approaches. Of the approximate 180 SeaSondes operating along US West coast and in Asia, it is estimated that about 60% would be suitable for tsunami observation.

A magnitude 8.6 undersea earthquake struck off the Indonesian province of Aceh on Wednesday, 11 April 2012, at 8:38 UTC. Both the initial earthquake and the magnitude 8.2 aftershock shifted the crust on either side of the fault mostly horizontally, rather than vertically. The resulting tsunamis were much smaller than those generated by the 2004 Indonesia and the 2011 Japan earthquakes, which were caused primarily by vertical slippage. This paper documents detection of these weak tsunamis by HF radars and tide gauges on the coasts of Sumatra and the Andaman Islands. Locations of the earthquake epicenters, radars and neighboring tide gauges are shown in Figure 1.

2. HF Radar Tsunami Detection

Barrick [8] originally proposed the use of shore-based HF radar systems for tsunami warning. Lipa *et al.* [9] described a simulation that superimposed modeled tsunami-induced currents at the end of the HF radar processing chain and proposed a detection method based on these simulations. Heron *et al.* [10] performed simulations addressing the detectability of tsunamis with HF radar, showing that a radar situated on the Great Barrier Reef is capable of monitoring small, as well as larger, tsunamis and has the potential to contribute to the understanding of tsunami genesis research. To achieve this, the HF radar would need to be switched to an alert mode of operation, presumably following a seismic event. Gurgel *et al.* [11] described a simulation study to estimate the tsunami-induced current velocity. This ocean current signal was then superimposed on HF radar backscatter signals, which then display specific radial tsunami current signatures. They described a tsunami detection algorithm that could be used to issue an automated tsunami-warning message.

Figure 1. Locations of the 8.6 and 8.2 magnitude earthquakes, occurring April 11 at 8:38 and 10:43 UTC, radars at Padang (PDNG), Hut Bay (HUTB), Port Blair (PTBL) and neighboring tide gauges (T.G.).

The analysis described in [9–11] is based on simulated tsunami currents, which at that time was the only data available. Since then we have accumulated a database of actual HF radar tsunami observations from both strong (Japan 2011) and weak (Indonesia 2012) tsunamis that can be used to test automatic detection methods more realistically. Signals generated by the Japan tsunami were observed to cause characteristic long-period oscillations in current velocities measured by high frequency radars [4,5]. We found that the methods described in [9] did not detect the tsunami signal in measured data from the Japan tsunami. A new tsunami detection algorithm was developed and

demonstrated offline to detect the arrival of the strong Japan tsunami in the coverage area of fourteen radars [12]. In this paper, we extend this analysis to the detection of weak tsunamis generated by the 2012 Indonesian earthquakes. Although these tsunamis were too weak to produce the large velocity oscillations that characterized the Japan tsunami, correlations between velocities at different ranges allowed the tsunamis to be detected. Detection times at the radars are compared with arrival times measured by tide gauges in the area. These detection methods were applied offline. As stated earlier, real-time detection awaits the installation of tsunami detection software on the field radar systems

3. Data Sets

We analyzed data sets from a SeaSonde HF radar system located at Padang, Sumatra, and two others located at Hut Bay and Port Blair on the Andaman Islands. System specifications for the SeaSonde are available online [13].

Figure 2 shows the bathymetry offshore from the Sumatra and Andaman Islands radar sites. As a general rule, moderate sized tsunamis become visible to the radar when they enter water of depth less than 200 m within the radar coverage area. From the data in Figure 2 we estimate detection ranges for PDNG, HUTB, PTBL of 12 km, 20 km, 20 km respectively.

The Padang radar is situated approximately South-East of the earthquake epicenter and is partly shadowed from the tsunami by islands (Figures 1 and 2(a)). The Hut Bay radar is situated almost due North from the earthquake epicenter (Figure 1). The Port Blair radar is situated about 120 km North from Hut Bay (Figure 2(b)). Radar spectra files with 4-minute time resolution were analyzed in all cases. Port Blair spectra had low signal-to-noise ratio and there were time gaps in the data stream.

Figure 2. The bathymetry offshore from (**a**) PDNG, (**b**) HUTB, PTBL.

(**a**)

Figure 2. *Cont.*
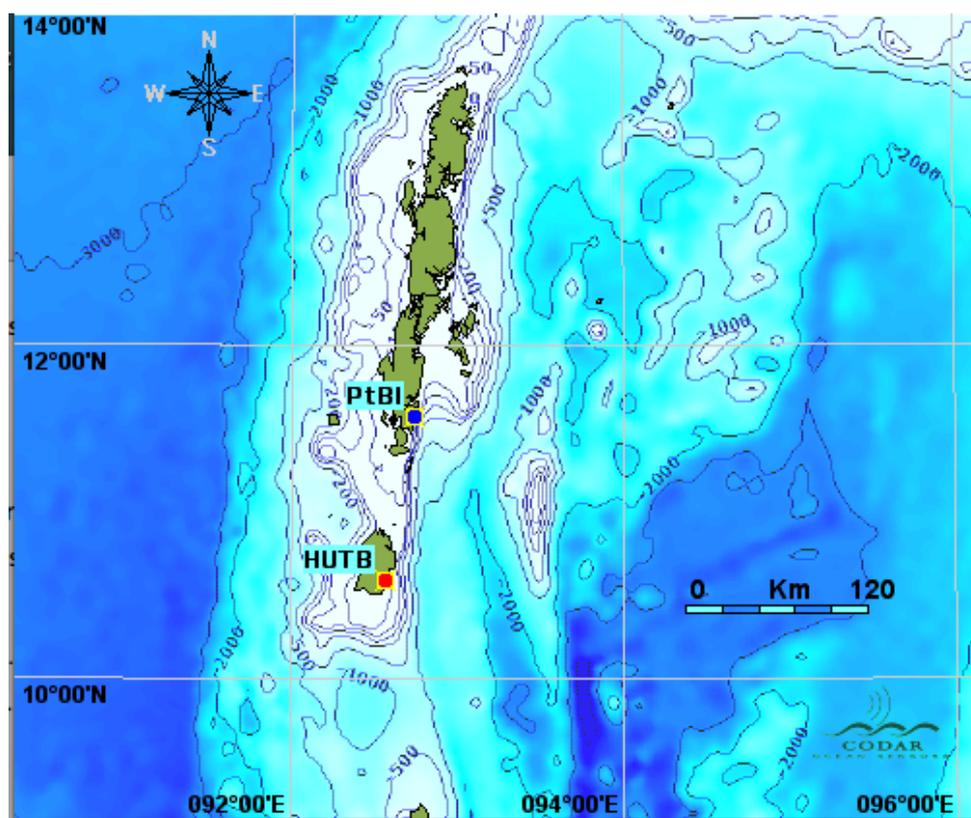
(b)

Table 1 shows the radar operating frequencies, range cell widths and the observation periods for the three radars.

Table 1. Radar parameters and data dates.

Radar Location	Frequency (MHz)	Range Cell Width (km)	Data Period 11 April 2012
Padang	14	3	06:00–14:21 UTC
Hut Bay	4.4	6	00:00–19:35 IST
Port Blair	4.4	6	00:00–20:42 IST

Radar results were compared with data from tide gauges at Sinabang, Teluk Bayur, Nancowry and Port Blair (Figure 1). The data from the Telukdalam tide gauge was not used, as it appeared to be defective, showing velocity oscillations with a period of about 5 min, which is atypical for a tsunami.

4. Methods

The methods described previously [12] were modified slightly to observe the tsunami signal. To summarize: (a) Short-term radar cross spectra (4-min time resolution) were analyzed to give radial velocities; (b) Radial velocities in narrow rectangular area bands approximately parallel to the depth contours were resolved parallel and perpendicular to the depth contour; (c) These velocity components were averaged within each band to reduce the noise that is inherent in velocities derived from short 4-min spectra.; (d) Time series of the average velocity components were formed.

For the strong Japan tsunami [4,12] two effects distinguished the velocities from the background: (i) after arrival within the area monitored, velocities in neighboring bands were strongly correlated and

(ii) the oscillation magnitudes deviated significantly from background values. For the weak Indonesia tsunamis, velocity oscillation magnitudes did not deviate significantly from the background: it is the correlations between velocities in different bands that allow the tsunamis to be detected. We used the pattern detection procedure developed for the Japan tsunami [12] to calculate a factor (the q-factor) that signals the tsunami arrival when it exceeds a preset threshold. For this study, the threshold was set to 500. The tsunami signal can be evident for some time after arrival; the detection method is optimized to apply to the first arrival.

These detection methods were applied offline. Real-time detection awaits the installation of tsunami detection software on the field radar systems.

5. Results

5.1. Observation and Detection at Padang, Sumatra

The tsunami arrival signature was observed in the velocity component parallel to the coast. This may be due to the tsunami approach predominantly parallel to the coast as might be expected given the locations shown in Figure 1.

Figure 3. PDNG radar observations 11 April 2012. (**a**) Velocity *vs.* time from 8:38 UTC. Blue: 0–2 km; Red: 2–4 km; Black: 4–6 km. (**b**) The q-factor corresponding to (a) displaying detections of both tsunamis. (**c**) Velocity *vs.* time from 8:38 UTC for 2 hours surrounding the arrival of the first tsunami. Blue: 0–2 km; Red: 2–4 km; Black: 4–6 km, showing the typical tsunami velocity arrival signature. (**d**) The q-factor corresponding to (c). (**e**) Velocity *vs.* time from 8:38 UTC for 2 hours surrounding the arrival of the second tsunami. Blue: 6–8 km; Red: 8–10 km; Black: 10–12 km, showing the typical tsunami velocity arrival signature. (**f**) The q-factor corresponding to (e).
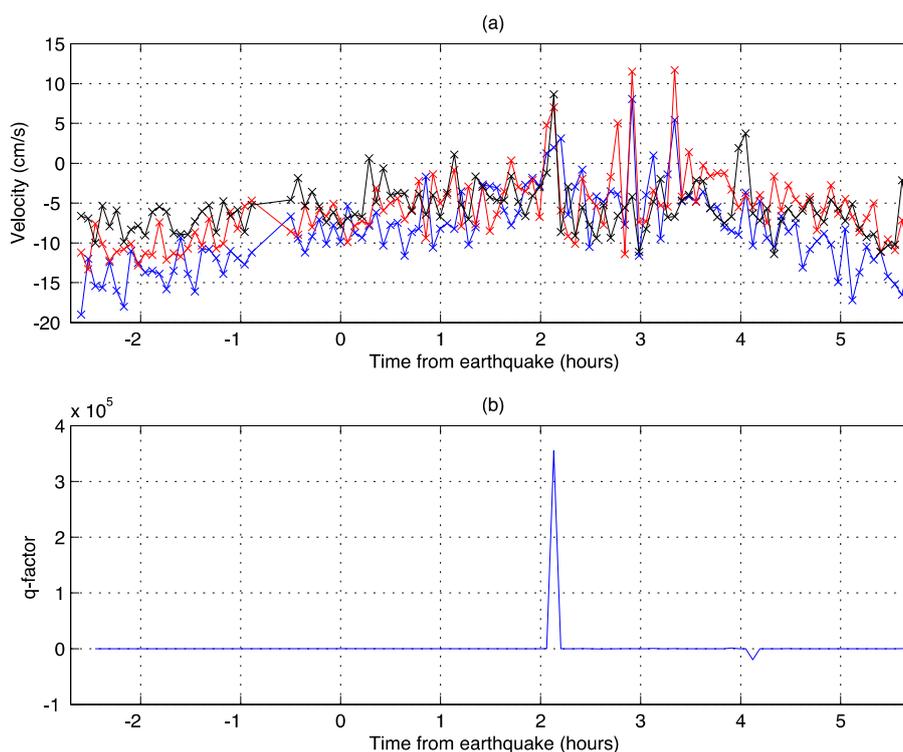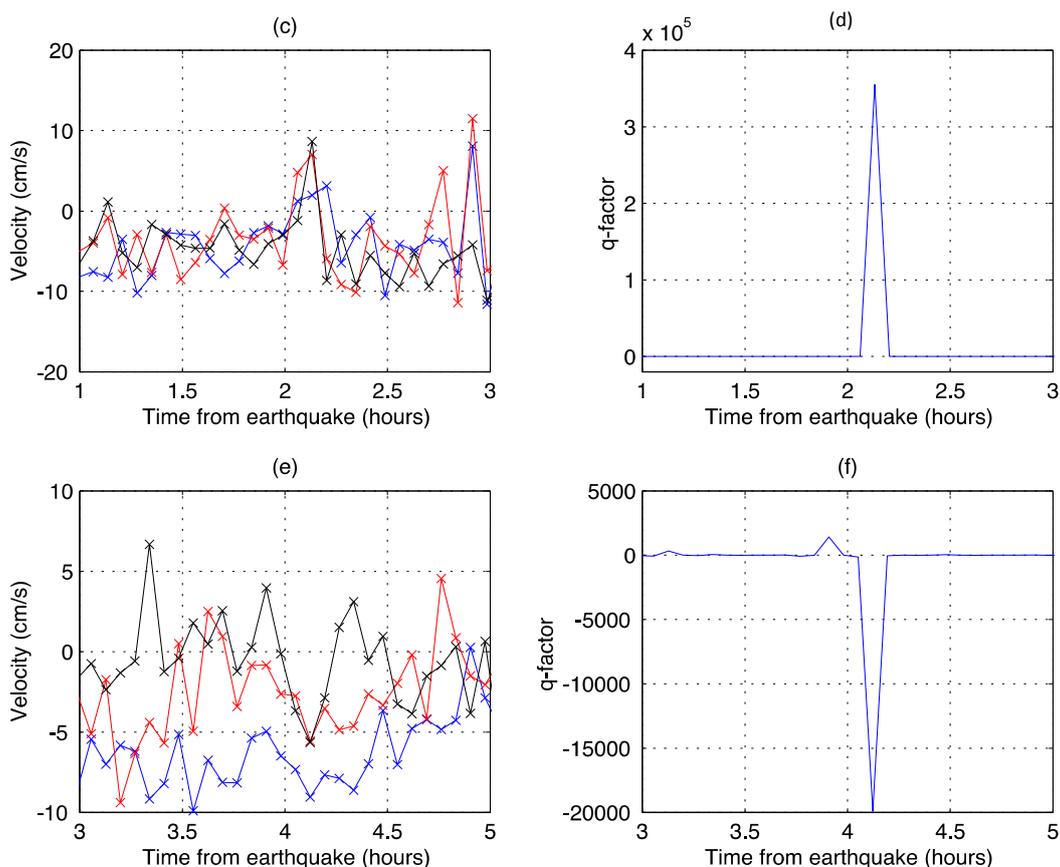
Figure 3. *Cont.*

Figure 3 shows the averaged velocities in three area bands 2-km wide and the corresponding q-factors. Tsunamis were detected following both the 8.6 magnitude earthquake occurring at 8:38 UTC, 2.31°N, 93.06°E and the 8.2 magnitude earthquake occurring at 10:43 UTC, 0.71°N, 92.45°E.

Figure 4. Tide gauge and q-factor observations 11 April 2012. (**a**) Tide gauge water levels. Blue: Sinabang, Red: Teluk Bayur (water levels are offset by −2 m to help with the plotting). The arrival of the first tsunami is indicated by '+'. (**b**) The q-factor from the PDNG radar.
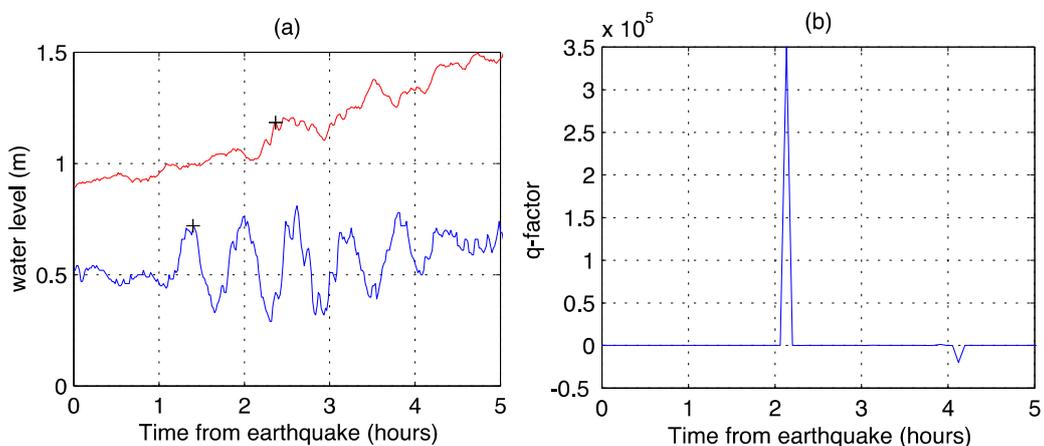

Figure 4 shows the water levels measured by a tide gauges at Sinabang, Teluk Bayur and the q-factor measured at PDNG for a 5-hour period. The closest tide-gauge to PDNG is Teluk Bayur,

approximately 15 km south. The arrival of the first tsunami is evident in the water levels; they do not show clearly when the second tsunami arrived.

Table 2 compares tsunami arrival times measured by the radar and by neighboring tide gauges and gives the tsunami height, which is taken to be the deviation from the background at arrival.

Table 2. Comparison of tsunami arrival times from the PDNG radar and neighboring tide gauges.

Instrument	Latitude	Longitude	Arrival Time 11 April 2012 UTC	Observed Tsunami Height (cm)
PDNG (radar)	−0.90	100.34	10:46, 12:33	
Sinabang (T.G.)	2.47	96.47	10:02	25
Teluk Bayur (T.G.)	−1.00	100.37	11:00	15

5.2. Observation and Detection at Hut Bay, Andaman Islands

Figure 5 shows the averaged velocities (perpendicular component) in three 6-km East-West bands and the corresponding q-factors. A tsunami was detected following the initial 8.6 earthquake. No signal was detected following the 8.2 aftershock.

Figure 5. HUTB radar observations 11 April 2012. (**a**) Velocity *vs.* time from 8:38 UTC. Blue: 6–12 km; Red: 12–18 km; Black: 18–24 km. (**b**) The q-factor corresponding to (a) with the tsunami arrival indicated by the first peak, followed closely by a smaller secondary peak. (**c**) Velocity *vs.* time for 1.5 hours surrounding the arrival of the tsunami: Blue: 6–12 km; Red: 12–18 km; Black: 18–24 km, showing the typical tsunami velocity arrival signature. (**d**) The q-factor corresponding to (c).
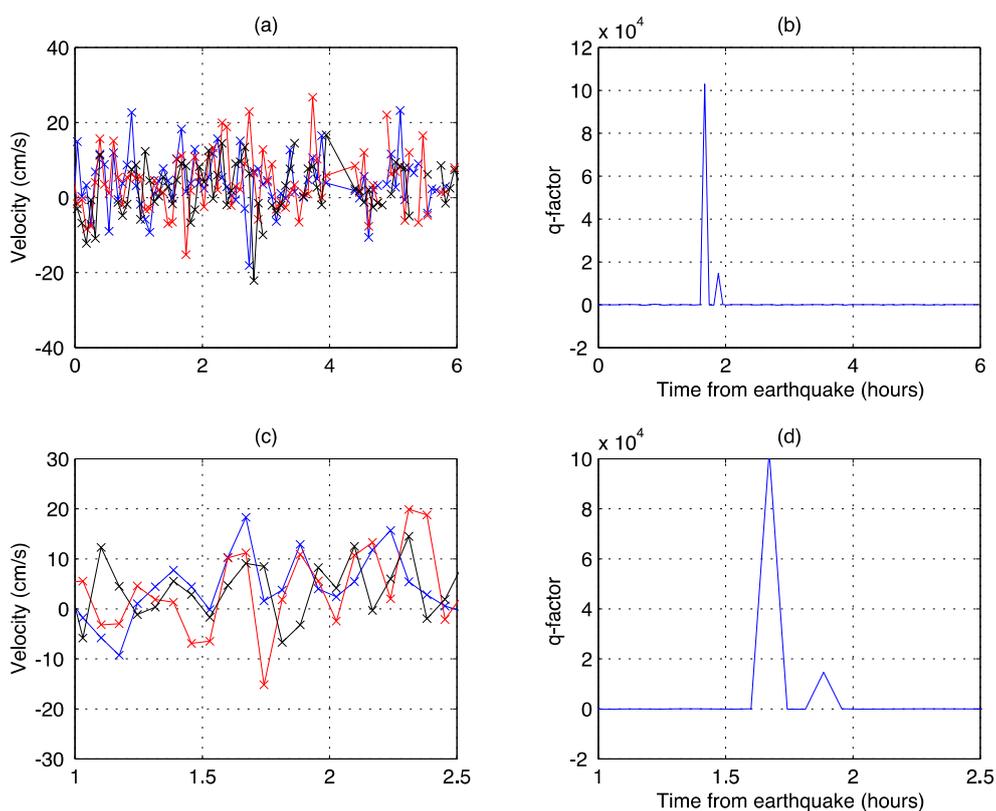
Figure 6 shows for a 5-hour period the water levels measured by tide gauges at Campbell Bay, Nancowry and Port Blair. The closest tide-gauge to HUTB is Port Blair approximately 124 km to the north.

Figure 6. Tide gauge and q-factor observations 11 April 2012. (**a**) Blue: Campbell Bay. Red: Nancowry, Black: Port Blair (water levels offset down by 0.55m to separate the curve from the others). The arrival of the tsunami is indicated by '+'. (**b**) q-factor from the HUTB radar. (**c**) Detail of Port Blair water levels. (**d**) Detail of HUTB q-factor.
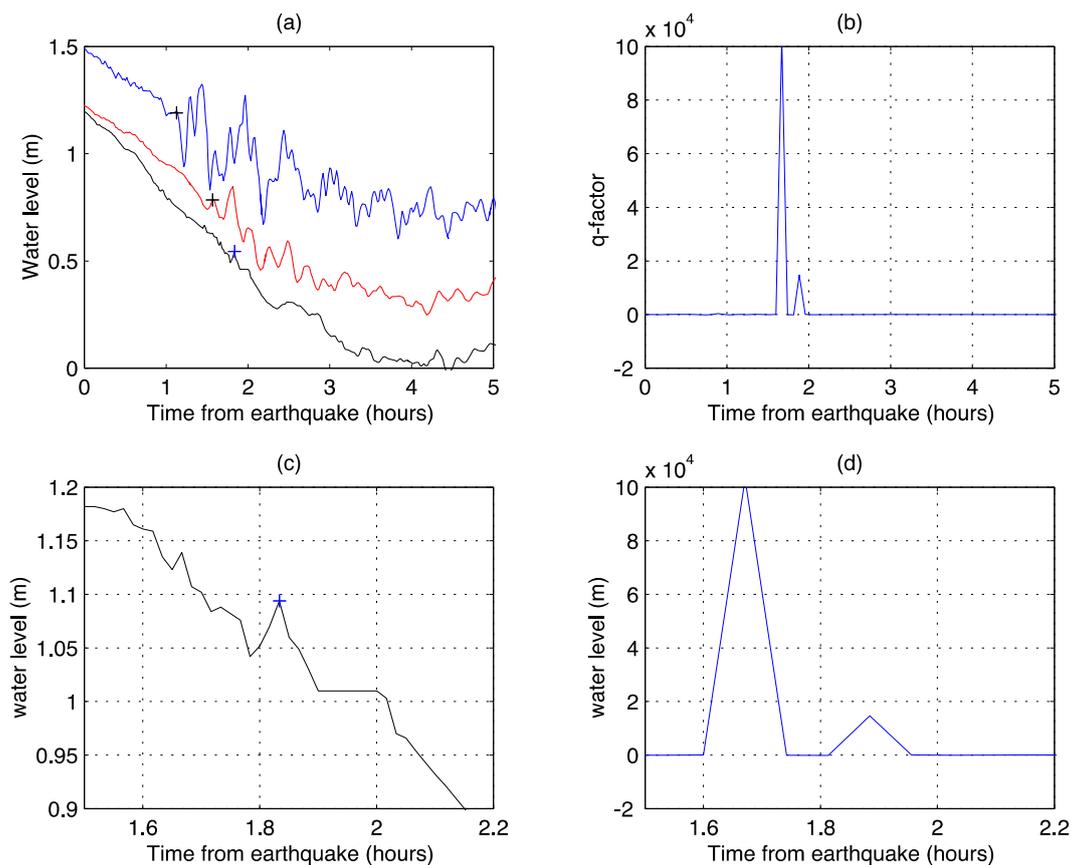

Table 3 compares tsunami arrival times measured by the radar and neighboring tide gauges and gives the tsunami height, which is taken to be the deviation from the background at arrival.

**Table 3.** Comparison of tsunami arrival times from the HUTB radar and neighboring tide gauges.

Instrument	Latitude	Longitude	Arrival time April 11 2012 UTC	Observed Tsunami Height (cm)
HUTB (radar)	10.59	92.55	10:18	
Campbell Bay (T.G.)	6.90	93.70	9:46	30
Nancowry (T.G.)	7.96	93.53	10:10	12
Port Blair (T.G.)	11.68	92.77	10:28	5

5.3. Observation at Port Blair, Andaman Islands

Figure 7 shows the averaged velocities (perpendicular component) in 6-km East-West area bands and the corresponding q-factors. The averaged velocity components in four adjacent bands appear to

show correlated peaks at 10:28 (1.83 hours after the 8.6 magnitude earthquake). However the correlation was too weak to trigger a tsunami detection.

Figure 7. PTBL radar observations 11 April 2012. (**a**) Velocity *vs.* time from 8:38 UTC. Blue: 0–6 km; Red: 6–12 km; Black: 12–18 km. (**b**) The q-factor corresponding to (a). (**c**) Velocity *vs.* time for 1.5 hours surrounding the arrival of the tsunami. Blue: 0–6 km; Red: 6–12 km; Black: 12–18 km, Green: 18–24 km, showing correlated peaks at the 10:28, followed by a data gap. (**d**) The q-factor corresponding to (c).
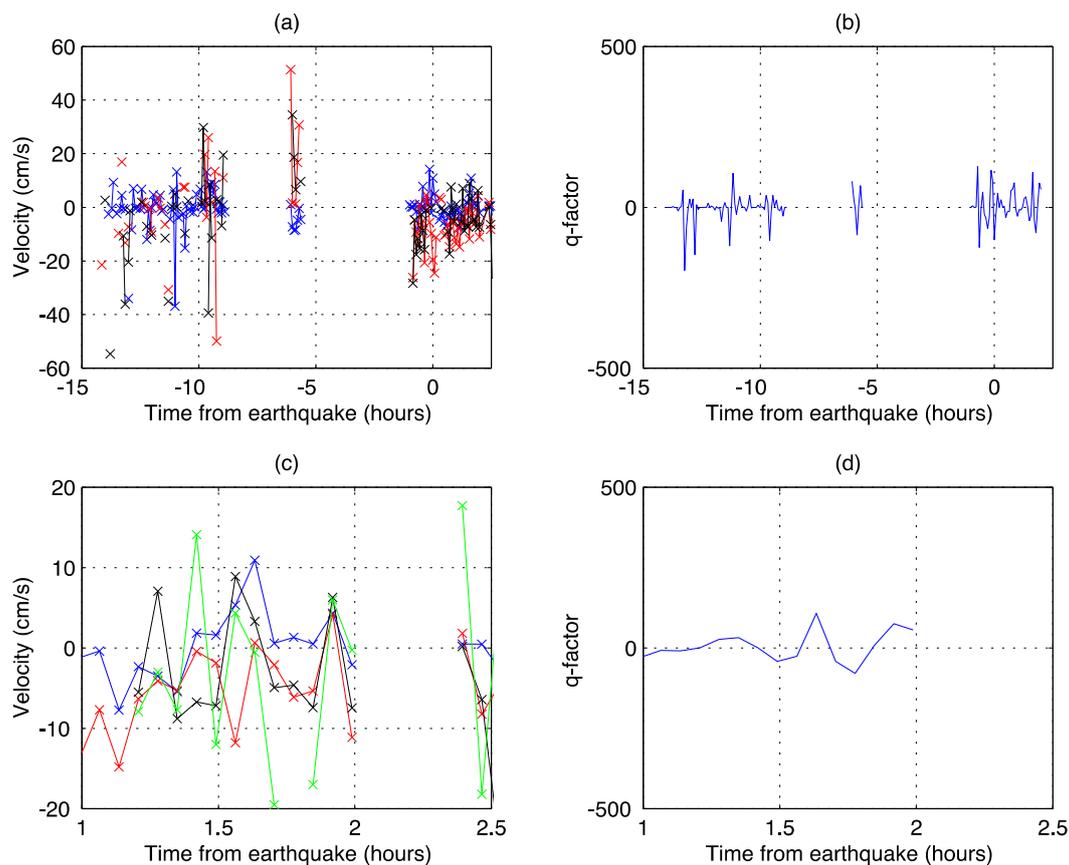
6. Discussion

The detections of the strong Japan [12] and weak Indonesia tsunamis reported here are the first studies indicating that actual tsunami arrivals can be detected in measurements made by coastal HF radars following major earthquakes. Previous studies [9–11] were based on simulated data.

The tsunami arrived at the Port Blair tide gauge only 18 minutes after the arrival at Nancowry. Direct travel between these sites would indicate an impossibly high speed of 1,406 km/h. Therefore, it appears that the tsunami approach to Port Blair is not directly from Nancowry but involves passage over deep-water regions where the speed is greater. Figure 1 shows that a direct path from the epicenter to Port Blair is over deep water much of the way, while the direct path from Nancowry is over shallower water. The mean tsunami speed from the epicenter to Port Blair along a direct path is a more reasonable 570 km/h.

The warning time provided by the radar at Hut Bay is somewhat uncertain, as there the tsunami height is low (Table 3). Taking the arrival at the Port Blair tide gauge to be signaled by the 5 cm

water-level peak at April 11 10:28 UTC (Figure 6), the radar saw the tsunami 10 min before it arrived at the tide gauge 124 km away. The Padang radar saw the tsunami with 14 min warning, shown by comparing the arrival times at the radar and the neighboring Teluk Bayur tide gauge, 15 km away. This is in an area with almost no continental shelf. The tsunami height was only 15 cm (Table 2).

It is evident from Figures 3(b), 5(b) and 7(b) that there were no false alarms for the data from Indonesia and the Andaman Islands used for this study, as the times when the q-factor exceeds the preset threshold are closely correlated with the earthquake occurrence, indicating the tsunami arrival. In addition, q-factor results from data measured by fourteen HF radar sites in Japan and USA on 11 March 2011 [12] showed only one false alarm over approximately 200 h of observations before the arrival of the Japan tsunami.

7. Conclusions

This paper demonstrates that the detection algorithm originally developed for the devastating 2011 Japan tsunami [12] successfully detected the weak 2012 Indonesia tsunami with only slight modification. These detections of the Japan and Indonesia tsunamis are the first demonstration that tsunami arrivals can be detected in coastal high frequency (HF) radar measurements, albeit not in real time. Tsunami velocities have a characteristic oscillatory behavior and velocities in neighboring locations are strongly correlated. We describe and demonstrate an empirical detection method based on these tsunami characteristics. We find that tsunami arrival within the radar coverage area can be announced approximately 8 min (*i.e.*, twice the radar spectral time resolution) after its first appearance. This can provide advance warning of the tsunami approach to the coastline locations when the water depth is less than 200 m. We note that the initial water-height increase due to the Indonesia tsunami as measured by the tide gauges was small, ranging from 5 to 30 cm. Thus it appears possible to detect even weak tsunamis using this method. Larger tsunamis could obviously be detected further from the coast, with increased warning times.

False alarms are to be expected when any empirical signal detection algorithm is applied to noisy data. Improved understanding of the false alarm rate will be possible when the deployment of tsunami detection software on field systems is complete. The software will run continuously in the background and any false alarm will be noted. The empirical detection algorithm will be modified to reduce the false-alarm rate while preserving the tsunami detection. An immediate improvement is expected when velocities within site-specific bathymetric contours are used for tsunami analysis rather than fixed rectangular bands used at present. In addition, statistics will be improved when multiple sites cover a common area. A promising deterministic approach is to look for pre-determined tsunami spatial patterns in radial current velocities [14]. These spatial patterns are derived from analytical models based on local bathymetry and shoreline configuration. This more sophisticated technique is under development.

The present tsunami arrival signals were visible only a short time before impact on the shore. This is due both to the narrow offshore shallow-water shelf and the low height of the tsunami. Nevertheless, the results show promise for improved offshore detection especially for destructive tsunamis with heights of 1 m or more. Using similar methods in ongoing studies, we can now provide accurate estimates of the observation/warning times for other regions, e.g., the US east coast, South East Asia and the west coast of India, where shallow-water bathymetry extends well offshore. HF radar

installations at such locations will provide vital capability for the detection and measurement of the local intensity of deadly approaching tsunamis as well as detailed comparisons between observation and model predictions.

HF radar systems are already in place at many coastal locations around the world to monitor surface currents and waves. Tsunami-watch software will run in the background, activating a warning should a tsunami be detected, before local infrastructure is damaged.

Acknowledgments

References

1. Titov, V.V. Tsunami Forecasting. In *The Sea*, Chapter 12; Harvard University Press: Cambridge, MA, USA, 2009; Volume 15, pp. 371–400.
2. Wei, Y.; Bernard, E.N.; Tang, L.; Weiss, R.; Titov, V.V.; Moore, C.; Spillane, M.; Hopkins, M.; Kânoğlu, U. Real-time experimental forecast of the Peruvian tsunami of August 2007 for US coastlines. *Geophys. Res. Lett*. **2008**, *35*, L04609.
3. Titov, V.V.; González, F.I.; Bernard, E.N.; Eble, M.C.; Mofjeld, H.O.; Newman, J.C.; Venturato, A.J. Real-time tsunami forecasting: Challenges and solutions. *Natural Hazards* **2005**, *35*, 41–58.
4. Lipa, B.; Barrick, D.; Saitoh, S.-I.; Ishikawa, Y.; Awaji, T.; Largier, J.; Garfield, N. Japan tsunami current flows observed by HF radars on two continents. *Remote Sens.* **2011**, *3*, 1663–1679.
5. Hirofumi, H.; Fujii, S., Furukawa, K.; Kataoka, T.; Miyata, M.; Kobayashi, T.; Mizutani, M.; Kokai, T.; Kanatsu, N. Propagating tsunami wave and subsequent resonant response signals detected by HF radar in the Kii Channel, Japan. *Estuar. Coastal Shelf Sci.* **2011**, 95, 268–273.
6. Kaplan, D.M.; Largier, J.L.; Botsford, L.W. HF radar observations of surface circulation off Bodega Bay northern California, USA. *J. Geophys. Res.* **2005**, *110*, C10020.
7. Kaplan, D.M.; Largier, J.L. HF-radar-derived origin and destination of surface waters off Bodega Bay. *Deep Sea Res. II* **2006**, *53*, 2906–2930.
8. Barrick, D.E. A coastal radar system for tsunami warning. *Remote Sens. Environ.* **1979**, *8*, 353–358.
9. Lipa, B.; Barrick, D.; Bourg, J.; Nyden, B. HF radar detection of tsunamis. *J. Oceanogr.* **2006**, *2*, 705–716.
10. Heron, M.L.; Prytz, A.; Heron, S.F.; Helzel, T.; Schlick, T., Greenslade, D.J.M.; Schulz, E.; Skirving, W.J. Tsunami observations by coastal ocean radar. *Int. J. Remote Sens.* **2008**, *29*, 6347–6359.
11. Gurgel, K.-W.; Dzvonkovskaya, A.; Pohlmann, T.; Schlick, T.; Gill, E. Simulation and detection of tsunami signatures in ocean surface currents measured by HF radar. *Ocean Dyn.* **2011**, *61*, 1495–1507.
12. Lipa, B.; Isaacson, J.; Nyden, B.; Barrick, D. Tsunami arrival detection with High Frequency (HF) radar. *Remote Sens.* **2012**, *4*, 1448–1461.
13. Codar Ocean Sensors. *SeaSonde*; Available online: http://www.codar.com/SeaSonde.shtml (accessed on 28 August 2012).

14. Barrick, D.; Lipa, B.; Whelan, C. Bathymetric Influence on Tsunami Spatial/Temporal Patterns in HF Radar Currents. In *Proceedings of Oceans'12 MTS/IEEE Yeosu Conference*, Yeosu, Korea, 21–24 May 2012.